

# Ex Vivo Analysis of Kidney Graft Viability Using <sup>31</sup>P Magnetic Resonance Imaging Spectroscopy

Alban Longchamp, MD, PhD,<sup>1</sup> Antoine Klausner, PhD,<sup>2,3</sup> Julien Songeon, MS,<sup>2</sup> Thomas Agius, MS,<sup>1</sup> Antonio Nastasi, BS,<sup>4</sup> Raphael Ruttiman, BS,<sup>4</sup> Solange Moll, MD,<sup>5</sup> Raphael P. H. Meier, MD, PhD,<sup>4,6</sup> Leo Buhler, MD,<sup>7</sup> Jean-Marc Corpataux, MD,<sup>1</sup> and Francois Lazeyras, PhD<sup>2,3</sup>

**Background.** The lack of organs for kidney transplantation is a growing concern. Expansion in organ supply has been proposed through the use of organs after circulatory death (donation after circulatory death [DCD]). However, many DCD grafts are discarded because of long warm ischemia times, and the absence of reliable measure of kidney viability. <sup>31</sup>P magnetic resonance imaging (pMRI) spectroscopy is a noninvasive method to detect high-energy phosphate metabolites, such as ATP. Thus, pMRI could predict kidney energy state, and its viability before transplantation. **Methods.** To mimic DCD, pig kidneys underwent 0, 30, or 60 min of warm ischemia, before hypothermic machine perfusion. During the ex vivo perfusion, we assessed energy metabolites using pMRI. In addition, we performed Gadolinium perfusion sequences. Each sample underwent histopathological analyzing and scoring. Energy status and kidney perfusion were correlated with kidney injury. **Results.** Using pMRI, we found that in pig kidney, ATP was rapidly generated in presence of oxygen (100 kPa), which remained stable up to 22 h. Warm ischemia (30 and 60 min) induced significant histological damages, delayed cortical and medullary Gadolinium elimination (perfusion), and reduced ATP levels, but not its precursors (AMP). Finally, ATP levels and kidney perfusion both inversely correlated with the severity of kidney histological injury. **Conclusions.** ATP levels, and kidney perfusion measurements using pMRI, are biomarkers of kidney injury after warm ischemia. Future work will define the role of pMRI in predicting kidney graft and patient's survival.

## INTRODUCTION

The lack of available kidneys for transplantation is a major concern, responsible for excess in morbimortality, and cost to healthcare systems.<sup>1</sup> Thus, to expand the organ supply, a variety of efforts have been made, such as accepting organs from donors after circulatory death (DCD), or with comorbidities (extended criteria donors [ECDs]). However, their usage is limited, due mainly to the fact that there is no reliable, noninvasive means to assess graft viability ex vivo. Shockingly, in the United States, 18% of all donated kidneys and 45% of ECD kidneys were not allocated for transplantation, despite that such kidneys could have been transplanted with good outcomes.<sup>1,2</sup> In addition, the

introduction of policies that penalize centers with poor outcomes resulted in an increase in the number discarded marginal kidneys,<sup>3</sup> a practice called "risk-averse transplant behavior."<sup>4</sup>

A number of tools are used to predict the suitability of kidneys before transplantation. These include stratification of donors according to clinical parameters, risk scores, histological donor biopsy scores, machine perfusion characteristics, biomarkers, and so on.<sup>5</sup> Besides the dichotomous ECD classification,<sup>6</sup> none of the scoring tools are clinically used.<sup>7</sup> Consequently, transplant outcome remains difficult to predict based on current

Received 12 February 2020. Revision received 9 March 2020.

Accepted 24 March 2020.

<sup>1</sup> Department of Vascular Surgery, Centre Hospitalier Universitaire Vaudois and University of Lausanne, Lausanne, Switzerland.

<sup>2</sup> Department of Radiology and Medical Informatics, University of Geneva, Geneva, Switzerland.

<sup>3</sup> Center for Biomedical Imaging (CIBM), Geneva, Switzerland.

<sup>4</sup> Visceral and Transplant Surgery, Department of Surgery, Geneva University Hospitals and Medical School, Geneva, Switzerland.

<sup>5</sup> Division of Clinical Pathology, Department of Pathology and Immunology, Geneva University Hospital and Medical School, Geneva, Switzerland.

<sup>6</sup> Department of Surgery, University of Maryland School of Medicine, Baltimore, MD, USA.

<sup>7</sup> Faculty of Science and Medicine, Section of Medicine, University of Fribourg, Switzerland.

This work was supported by the Swiss National Science Foundation to J.-M.C., F.L. (SNSF 320030-182658), and A.L. (SNSF PZ00P3-185927) as well as the Mendez National Institute of Transplantation, and the Leenards Foundation to A.L.

The authors declare no conflicts of interest.

A.L., A.K., J.S., T.A., L.B., J.-M.C., and F.L. participated in research design. A.L., A.K., R.M., and F.L. participated in the writing of the article. A.L., A.K., J.S., T.A., A.N., R.R., S.M., R.M., J.-M.C., and F.L. participated in the performance of the research. A.N., R.R., S.M., and F.L. contributed new reagents or analytic tools. A.L., A.K., J.S., T.A., S.M., R.M., L.B., J.-M.C., and F.L. participated in data analysis.

Correspondence: François Lazeyras, PhD, Hôpitaux Universitaires de Genève, Service de Radiologie, CIBM Rue Gabrielle-Perret-Gentil 4, CH, 1211 Genève 14, Switzerland. (francois.lazeyras@unige.ch).

methods, and useful predictors of outcome that incorporate tissue viability are urgently needed.

The importance of energy metabolism, by which living cells acquire, and use the energy needed to stay alive, during organ transplantation has been duly acknowledged.<sup>8</sup> Consequently, current methods of organ preservation aim to preserve the energy machinery<sup>9</sup> and reduce the rate energy depletion.<sup>10</sup> The consensus is that a period of warm ischemia (>30 min in human kidney<sup>11</sup>), primes the tissue for subsequent damage upon reperfusion. During ischemia, ATP depletion disrupts mitochondrial Na<sup>+</sup>/K<sup>+</sup> ion channels, which reduce mitochondrial membrane potential and increase mitochondrial inner membrane permeability, influx of calcium ions, and subsequent swelling of mitochondria.<sup>12</sup> Once energy levels have fallen beyond a critical point, the resulting injury is irreversible.<sup>13</sup> Respiratory defects were identified as early events of injury during preservation<sup>13</sup> and after ischemia-reperfusion.<sup>14</sup> In livers, ATP content correlated with transplant outcome.<sup>15,16</sup> Unfortunately, clinical applicability of ATP measurement has been limited by time-consuming, invasive, and costly methods of ATP analysis.<sup>9</sup>

Magnetic resonance imaging (MRI) is well established as a clinical diagnostic modality. Kidney perfusion can be assessed by dynamic MRI using the first passage of Gadolinium (Gd)-chelate bolus.<sup>17</sup> Abnormal Gd uptake may also reflect arterial stenosis, glomerular filtration dysfunction,<sup>18</sup> and ischemia.<sup>19</sup> In addition to imaging the hydrogen nucleus, MRI enables detection of high-energy phosphate metabolites (<sup>31</sup>P MRI [pMRI] spectroscopy), such as ATP, phosphomonoesters (PMEs, that contain the ATP precursor AMP), phosphodiesteres, and phosphocreatine. Therefore, this method could be particularly suitable for monitoring tissue function and graft viability during transplantation.

Here, we demonstrate that using pMRI, ATP can be quantified ex vivo in kidney graft. Importantly, kidney ATP levels significantly correlated with graft Gd perfusion, and tissue injuries after warm ischemia. Thus, pMRI could facilitate rapid, and accurate assessment of kidney viability, with the hope to predict survival of kidney recipients.

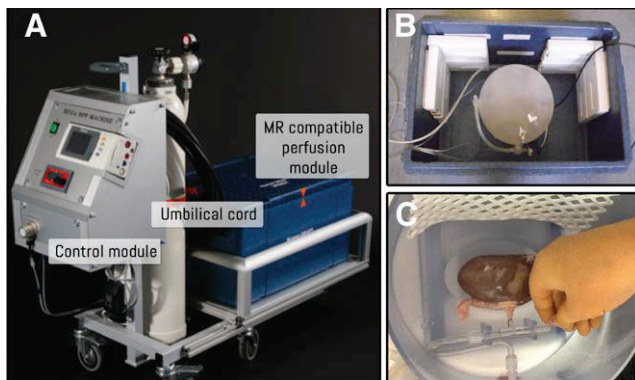


**FIGURE 1.** The homemade MR-compatible kidney ex vivo perfusion system. (A) The system is made of a control module to drive the pulsating pump and regulate the oxygenator, a perfusion tank containing the kidney graft, and linked through the umbilical cord. Compatible perfusion module fits in the MRI bore with a maximum size of 40 cm. (B, C) Inside view of the perfusion tank (B) with the kidney artery connected to a cannula (C). MRI, magnetic resonance imaging.

## MATERIALS AND METHODS

### Ex Vivo Hypothermic Oxygenated Pulsatile Perfusion

Kidneys were perfused by a homemade MRI-compatible machine with Belzer MPS UW Machine Perfusion Solution, and kept at 4°C for up to 22 h. All of the experiments were performed in presence of oxygen (100 kPa), as we previously demonstrated that the ability of the kidney to generate ATP relies on sufficient oxygenation.<sup>20</sup> The perfusion module, and its cooling box were MRI compatible. During the MRI acquisition, the control module was kept outside of the Faraday cage and was connected through the wall with an “umbilical cord,” that ensured adequate kidney oxygenation (Figure 1) and pulsatile perfusion. Systolic and diastolic pressure were set at 50 and 15 mmHg, respectively. Measurements were performed on a multi-nuclear Prisma-fit 3T whole-body MRI scanner (Siemens, Erlangen, Germany). Kidney localization was performed with a T2-weighted sequence (turbo spin echo, repetition time (TR) 5000 ms, echo time (TE) 108 ms, 3-mm slices).

### Gadolinium Perfusion

Gd perfusion enables the observation of the internal distribution of the flow between the cortex and the medulla. Low molecular weight Gd has a predominant renal elimination by glomerular filtration without any tubular secretion or reabsorption. Having a similar pharmacokinetics as tracer, they allow glomerular filtration rate assessment with MRI. The perfusion-descending cortical slope (DS) is evaluated with the elimination of the Gd using the angle between the maximum signal value in the cortex and the lowest intensity point at the end of the flushing (around 200 s).<sup>21</sup> In this study, 5 mL (0.025 mmol/mL) Gd-diethylenetriaminepentaacetic acid bolus injection was used for the renal perfusion (at 4°C), followed by a 20-mL flush of MP Belzer. The perfusion is a fast sequence, as data were collected using a dynamic 2D saturation-prepared turbo flash sequence with the scanner body coil. This sequence has an inversion time of 240 ms, a flip angle of 12°, 1.0 mm × 1.3 mm resolution, 5 slices of 5 mm (1-mm gap), TR 460 ms, and a TE of 1.3 ms.

### <sup>31</sup>P Magnetic Resonance Imaging Spectroscopy

pMRI was performed with a single-loop coil tuned at 49.5 MHz, which was part of the perfusion machine, as it was fixed at the bottom of the perfusion tank. The coil was interfaced with a specially designed transceiver that allows both 1H imaging and <sup>31</sup>P spectroscopy (Clinical MR Solutions, Brookfield, WI). The field homogeneity was optimized with automatic shimming over the kidneys. pMRI consisted of 3D spatial encoding, with a field of view 250 mm × 250 mm × 160 mm, matrix size 16 × 16 × 8, nominal spatial resolution 15.6 mm × 15.6 mm × 20 mm, TR 1.0 s, flip-angle 45°, echo delay 0.6 ms, bandwidth 4000 Hz, 2k sampling points. Elliptical encoding with 32 weighted averages, resulted in an acquisition time of 45 min. Chemical shift signal was referenced to the inorganic phosphate (Pi) resonance at 5.2 ppm, which can be considered homogeneously distributed over the surface of the coil. A frequency offset of -500 Hz was used to center excitation pulse bandwidth over ATP frequency range. Afterward, the spectrum was processed with a 20-Hz exponential time filter, and order 0 and 1 phase corrections. The metabolites (ATP,

PME, Pi, phosphocreatine) were fitted with Gaussian peaks using the syngo software (SIEMENS, Erlangen, Germany) and were estimated over all the kidneys by averaging pMRI voxels containing kidney tissue (combined voxels resulting in a single spectrum).  $\alpha$ ,  $\beta$ , and  $\gamma$  ATP correspond to the resonances of the  $3^{31}\text{P}$  nuclei contained in ATP. All 3 peak amplitudes are proportional to the ATP concentration but were quantified separately to prevent methodological bias. Indeed the excitation pulse profile might vary over the large frequency range spanned by the 3 peaks, and their quantification might be influenced by overlaps with other metabolite like nicotinamide adenine dinucleotide (NAD) (discussed further in the text). The metabolite concentrations were obtained as previously described.<sup>20</sup> Briefly,  $[\text{}^{31}\text{P}_m]$ , expressed as mmol/L (mM), was calculated using the following formula:  $[\text{}^{31}\text{P}_m] = (S_m/S_{\text{bPi}}) \times [\text{}^{31}\text{P}_{\text{buffer}}] \times C_{\text{sens}}$ , where  $S_m$  and  $S_{\text{bPi}}$  are the mean metabolite and buffer Pi signals (area), respectively.  $[\text{}^{31}\text{P}_{\text{buffer}}]$  is the buffer phosphate concentration (25 mmol/L).  $C_{\text{sens}}$  is the sensitivity correction factor.

### Animals

The study was approved by the University of Geneva animal ethics committee (protocol number: GE/53/14/22826). Five-month-old female pigs were obtained from the animal facility of Arare, Switzerland. All pigs were maintained under standard conditions. Water and food were provided ad libitum. Animals were first premedicated using azaperone (2.2 mg/kg IM), midazolam (1.6 mg/kg IM), and atropine (0.02 mg/kg IM) and anesthetized with ketamine (2–6 mg/kg/h), fentanyl (4–6  $\mu\text{g}/\text{kg}/\text{h}$ ), midazolam (0.2–0.4 mg/kg/h), and atracurium (1 mg/kg/h). Animals were then intubated and ventilated before a nasogastric tube was placed. The arterial line was placed in the internal carotid artery. Monitoring included heart rate, systemic blood pressure, pulse oximetry, and end-tidal  $\text{CO}_2$ . Following a midline incision, the peritoneal cavity was opened, and the bowels were retracted. First, the aorta, vena cava, and renal vessels were prepared. The pigs received 300 UI/kg heparin intravenous injections. Renal arteries and veins were clamped, and the kidneys were either immediately explanted or explanted after 30 and 60 min of warm ischemia (to mimic circulatory arrest during DCD procurement). Kidneys were then instantly flushed with 4°C Institut Georges Lopez-1 preservation solution on ice. Surgical kidney biopsies, including the cortex and the medulla, were formalin fixed and embedded in paraffin. The renal artery was cannulated, and the kidneys were cold perfused using our MR-compatible machine (Figure 1) before imaging. Pigs were sacrificed using 100 mEq of potassium chloride intravenous injections.

### Histopathological Analysis of Biopsies

Sections of 3- $\mu\text{m}$  thickness were prepared from formalin-fixed kidney biopsies and stained with silver Jones and Periodic Acid-Schiff. Histopathological analysis score was performed based on those described by Goujon et al<sup>22,23</sup> using Osirix software (www.osirix-viewer.com) and modified as previously described.<sup>22,24</sup> Four different representative fields were assessed and blinded to group assignment. Lesion severity was graded 0–5 according to the following criteria: no abnormality (0), mild lesions affecting, respectively, 1%–10% (1), 10%–25% (2), 25%–50% (3),

50%–75% (4), and >75% (5) of the sample surface. The final score for each biopsy ranges from 0 to 30. A higher score corresponding to the more severe ischemic damage.

### Statistical Analysis

The statistical tests used are defined for each figure in the appropriate legend. A  $P$  value <0.05 was considered statistically significant. Computations were performed using Prism 7 (GraphPad Softwares, San Diego, CA).

## RESULTS

### Kidney ATP Is Rapidly Generated During Ex Vivo Perfusion

Kidneys were perfused using a homemade MRI-compatible, hypothermic-oxygenated pulsatile perfusion machine (Figure 1). During the ex vivo perfusion, kidney metabolites were estimated by averaging pMRI voxels, resulting in a single spectrum (Figure 2A and B). In healthy kidneys (0 min of warm ischemia), pMRI allowed the detection of  $\alpha$ -,  $\beta$ -, and  $\gamma$ -ATP, PME and inorganic phosphate (Pi, Figure 2B). ADP was below the detection threshold. ATP and PME concentration (mM) were extrapolated from their spectra peak area and the buffer phosphate concentration (Pi, 25 mmol/L). In absence of warm ischemia, kidney  $\alpha$ -,  $\beta$ -, and  $\gamma$ -ATP, remained stable up to 22 h of perfusions (Figure 2C). On the other hand, PME concentration was 4 times higher than ATP at the initiation of the perfusion but gradually declined over time (Figure 2C). This is consistent with the hypothesis that the PME containing AMP signal is utilized over time to generate ATP.

### Warm Ischemia Reduces Kidney ATP Levels

To determine the effect of warm ischemia and to ensure sufficient sensibility of ATP measurement using pMRI in injured grafts, kidneys underwent 0 (control), 30 or 60 min of warm ischemia before retrieval. There was a significant reduction in the amount of  $\beta$ -ATP after 30 min (–48.4%;  $P=0.04$ ) and 60 min (–66.4%;  $P=0.007$ ) of warm ischemia (compared with no warm ischemia, Figure 3A). Similarly,  $\gamma$ -ATP was significantly decreased after 60 min of ischemia (–45.5%;  $P=0.05$ ; Figure 3A).  $\alpha$ -ATP did not significantly decrease, which could be explained by the presence of NAD overlapping at –8.3 ppm (Figure 3A). Since the peak of  $\alpha$ -ATP appears to be “contaminated” by NAD signal, ATP concentration was estimated by averaging  $\beta$ - and  $\gamma$ -ATP only. Compared with control, 60 min of warm ischemia induced a 58.5% fold reduction in total ATP (Student  $t$  test;  $P=0.03$ ). On the other hand, PME concentrations were not altered by warm ischemia (Figure 3B).

### ATP Levels and Kidney Perfusion Correlate With Histological Damage

To establish the relevance of ATP quantification using pMRI, we next examined the correlation with histological damage, as assessed by the Goujon score, which is thought to reflect kidney function.<sup>22</sup> As expected, 30 and 60 min of warm ischemia induced significant histological injuries (Figure 4A). Histological damages were quantified based on the number of tubules lumina with cellular debris, the loss of brush border, tubular dilatation, the percentage of flocculus in Bowman’s capsule, vacuolization, and

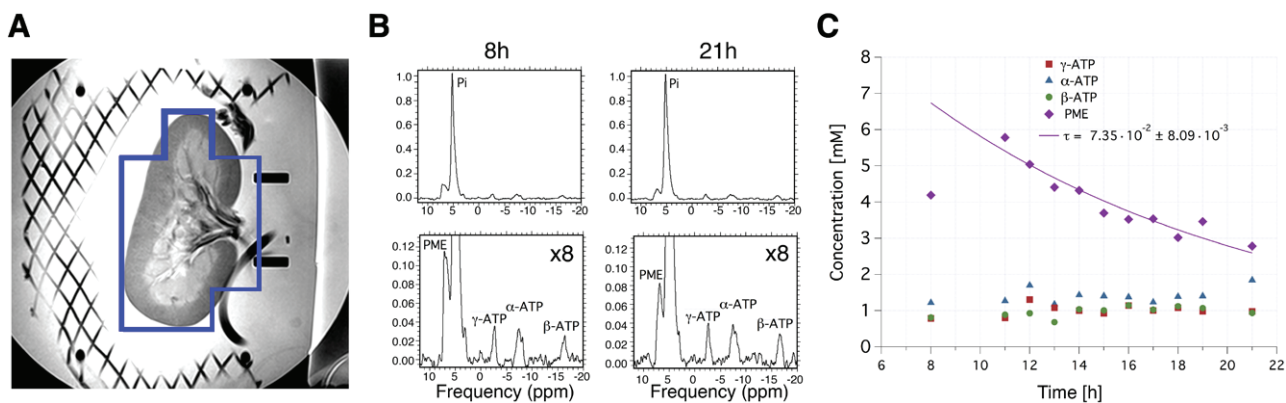


**FIGURE 2.** Representative pMRI spectra, and kidney ATP levels over time. (A) T2 image of a kidney, with the blue border representing the area of combined voxels that are analyzed for metabolite concentration. (B) Representative spectrum of kidney after 8 h (left) and 21 h (right) of hypothermic pulsatile perfusion. (C) Concentration (mM) of the indicated metabolites over time, in pig kidney, after 0 min of warm ischemia, during hypothermic pulsatile perfusion with a fixed  $pO_2$  of 110 kPa. pMRI,  $^{31}P$  magnetic resonance imaging; PME, phosphomonoester.

interstitial edema (Figure 4B), which were all increased by warm ischemia (except for vacuolization, Figure 4B). Of importance, the ability to produce ATP (Figure 4C and D) was tightly correlated with the degree of kidney injury (Figure 4D, Pearson's  $R^2=0.52$ ;  $P<0.001$ ). Histological injury did not correlate with PME levels (data not shown).

Gd perfusion enables the observation of flow between the cortex and the medulla, which was suggested to be altered during injury.<sup>21</sup> Consistent with our previous findings, kidney Gd cortex, and medulla perfusion were altered after 60 min of warm ischemia. This was reflected by a decrease in the DS (Figure 5A). Interestingly, kidney injury assessed using the cortex DS was significantly correlated with kidney ATP and with histological damage (Figure 5B and C; Pearson's  $R^2=0.64$  and  $0.43$ , respectively;  $P<0.001$ ). Thus, combining both ATP and DS measurements might allow the accurate prediction of kidney damage before transplantation.

## DISCUSSION

This study provides a noninvasive method to assess viability of kidneys ex vivo during hypothermic machine perfusion. In particular, the objective assessment of graft damage (eg, resulting from prolonged circulatory arrest,

DCD) could translate into greater utilization of kidney allograft.

Besides being used to reduce the risk of delayed graft function and improved graft survival after kidney transplantation,<sup>25</sup> machine perfusion enables viability testing by offering a dynamic environment. Various parameters have been proposed as predictive biomarkers, ranging from intrarenal resistance, markers of acid-base homeostasis, or lactate production.<sup>26</sup> Interestingly, we observed an exponential decrease of PME during the ex vivo perfusion, suggesting that AMP reserve contained in the PME metabolites is consumed to produce ATP. This is consistent with the idea that the kidneys are functionally and metabolically active in presence of oxygen.<sup>20,21</sup> In addition, there is emerging evidence that oxygenation is an important advantage during hypothermic machine perfusion.<sup>27,28</sup> Oxygen supplementation during organ preservation may drive ATP production through oxidative phosphorylation. Thus, cells can use ATP to sustain metabolic processes that protect from ischemic damage.<sup>29</sup> These further suggest the importance of functional mitochondria and the dependence on oxidative metabolism in healthy kidney. In addition, this suggests that kidney viability depends on the ability to generate ATP and not only the remaining

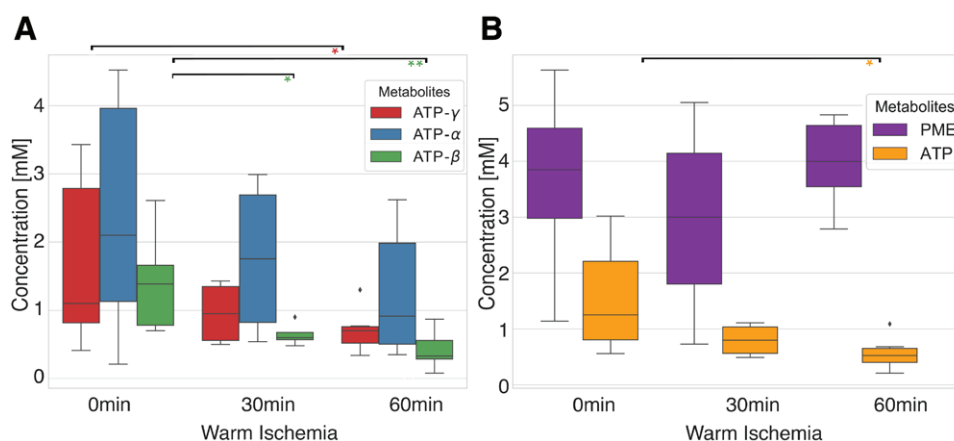


**FIGURE 3.** Kidney metabolite levels after 0, 30, and 60 min of warm ischemia. (A, B)  $\alpha$ -,  $\beta$ -, and  $\gamma$ -ATP expressed individually (A), and  $\beta$ - and  $\gamma$ -ATP combined and PME (B) following 0, 30, or 60 min of warm ischemia.  $n=4-9$  per group. Metabolites levels represent an average throughout perfusion. Error bars indicate SD \* $P<0.05$ , \*\* $P<0.01$ , by 2-way ANOVA. PME, phosphomonoesters.

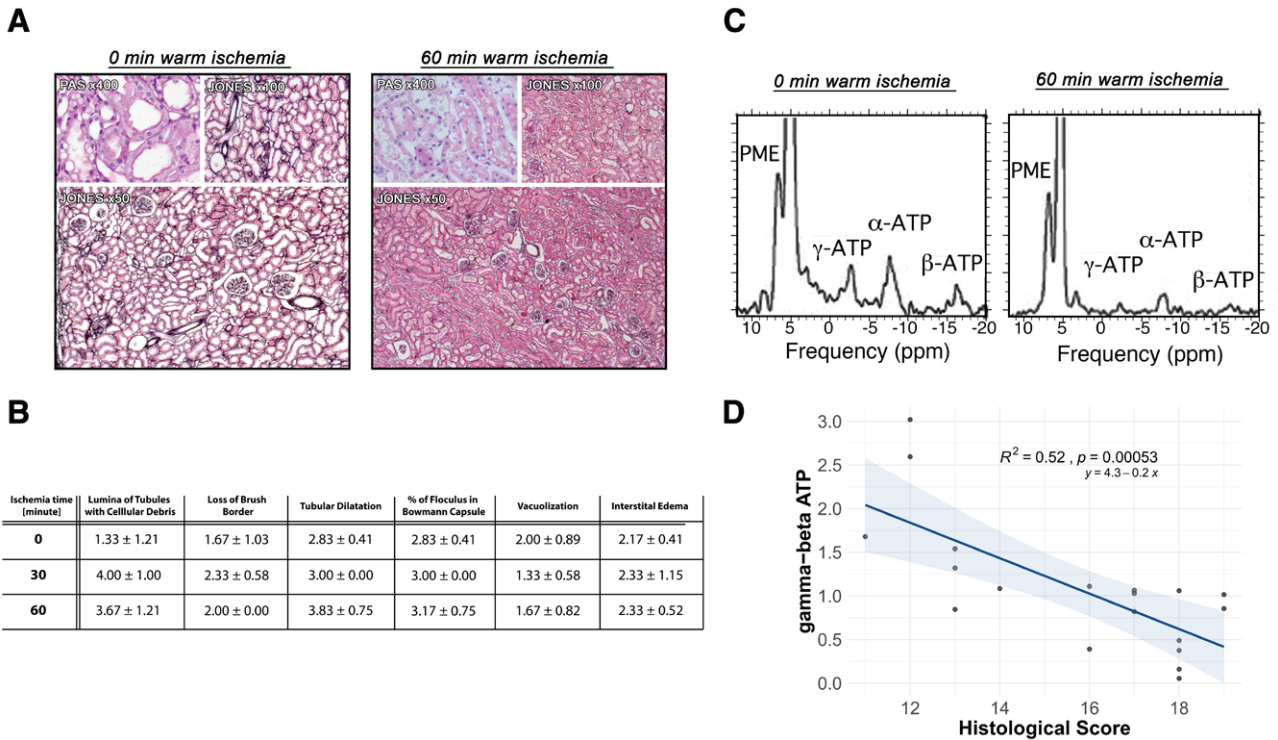


**FIGURE 4.** ATP levels correlate with histological damage. (A) Representative kidney sections stained with PAS or Jones after no (left) or 60 min (right) of warm ischemia. (B) Details of histological scoring after various warm ischemia time as indicated. Data are expressed as mean ± SD. (C) Representative MRI fitting spectra after no (left) or 60 min (right) of warm ischemia. (D) Nonparametric Spearman's correlation between kidney  $\gamma$ - and  $\beta$ -ATP and histological score after 0–60 min of warm ischemia with the coefficient of determination  $R^2$  and  $P$  value. Metabolites levels represent an average throughout perfusion.  $n = 27$ . MRI, magnetic resonance imaging; PAS, Periodic Acid-Schiff; PME, phosphomonoester.

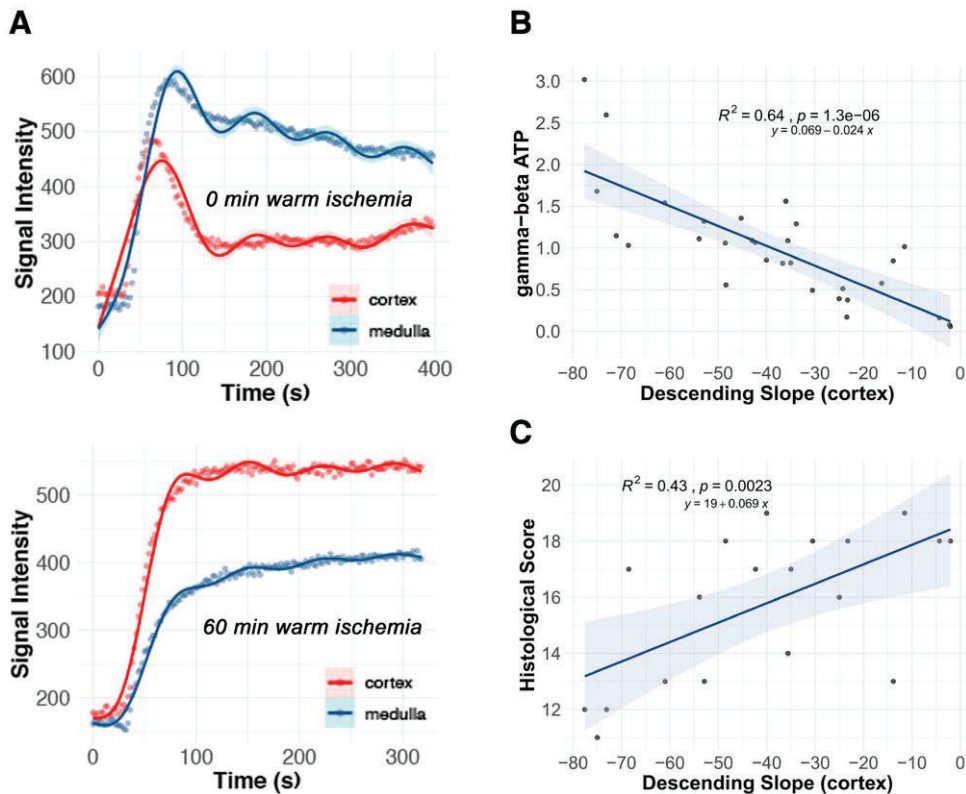


**FIGURE 5.** The perfusion-descending slope (DS) correlates with kidney ATP levels and histological damage. (A) Representative kidney Gd cortex (red line) and medulla (blue line) perfusion after no (top) or 60 min (bottom) of warm ischemia. (B, C) Unparametric Spearman's correlation between kidney cortex perfusion-descending slope, and  $\gamma/\beta$ -ATP (B) and with histological score (C) with their coefficient of determination  $R^2$  and  $P$  value,  $n = 27$ .

ATP store. Several studies demonstrated that ATP levels correlate with ischemic injury of the kidney<sup>30</sup> and liver.<sup>29</sup> Moreover, ATP is often used as a marker of viability during ischemia.<sup>31,32</sup> In humans, ATP level in liver tissue is an independent predictor of initial graft function.<sup>33</sup> Interestingly, ATP levels measured after transplantation were inversely related to warm ischemia time.<sup>16</sup> Similarly, low ATP levels were significantly associated with primary graft nonfunction.<sup>34</sup> Of importance, the inadequate recovery might be different in various marginal organs. For instance, ATP levels were lower in the DCD and steatotic livers.<sup>9</sup> Despite good correlation with outcome, energy status is difficult to measure, and yet to be used routinely for clinical testing. ATP measurements would be a precious addition to the pretransplant assessment of suboptimal organs, particularly in the setting of uncontrolled DCD procurement, where in the exact maximal donor warm ischemia duration is unknown, which is responsible for a large variation of acceptance criteria between centers.<sup>35</sup>

Our study has several limitations that need to be acknowledged. First, the broader utility of this methodology in determining graft viability should be tested in all form of marginal donor, including kidney from old donor, after acute kidney injury, and after prolonged cold preservation. In addition, we did not correlate ATP levels with kidney function in vivo, or after transplantation, mostly because of local regulation, that did not allow survival surgery. All of the above will hopefully be tested in a future human clinical trial. Although the histological score was not validated in a prospective human cohort, it was previously correlated with the degree of kidney injury.<sup>22-24</sup> The clinical use of pMRI might be limited by the time of acquisition (45 min). However, the acquisition was performed during the hypothermic ex vivo perfusion,<sup>27</sup> and the imaging time could be reduced either by reducing spatial encoding resolution or by using advanced method for fast spatial encoding.<sup>36</sup> In addition, the fitting of  $\alpha$ -ATP with a broad Gaussian probably includes the NAD<sup>+</sup> and NADH signal at  $-8.3$  ppm. Thus, the quantification of the pMRI spectra could be improved for overlapping metabolites, using a model that comprises each metabolite spectrum with multiplet structures. This could for instance allow for the specific detection of NAD<sup>+</sup>/H signal that is weak and overlaps with alpha-ATP peak.<sup>37</sup> Altogether, it is likely that the pMRI process can be integrated within the “normal” cold ischemia period.

In conclusion, pMRI performed on a kidney graft held in an ex vivo perfusion system produced excellent quality spectra. ATP levels and kidney perfusion measurements could accurately predict kidney damage caused by warm ischemia. In an era when up to 45% of ECD kidneys are discarded, this study provides a timely and innovative noninvasive tool to assess kidney viability before transplantation.

## ACKNOWLEDGMENTS

We thank Jean-Pierre Gilberto for his excellent technical assistance.

## REFERENCES

1. Hart A, Smith JM, Skeans MA, et al. OPTN/SRTR 2017 annual data report: kidney. *Am J Transplant.* 2019;19(Suppl 2):19–123. doi:10.1111/ajt.15274

2. Aubert O, Reese PP, Audry B, et al. Disparities in acceptance of deceased donor kidneys between the United States and France and estimated effects of increased US acceptance. *JAMA Intern Med.* 2019;179:1365–1374. doi:10.1001/jamainternmed.2019.2322.
3. Rege A, Leraas H, Vikraman D, et al. Could the use of an enhanced recovery protocol in laparoscopic donor nephrectomy be an incentive for live kidney donation? *Cureus.* 2016;8:e889. doi:10.7759/cureus.889
4. Heilman RL, Green EP, Reddy KS, et al. Potential impact of risk and loss aversion on the process of accepting kidneys for transplantation. *Transplantation.* 2017;101:1514–1517. doi:10.1097/TP.0000000000001715
5. Sung RS, Christensen LL, Leichtman AB, et al. Determinants of discard of expanded criteria donor kidneys: impact of biopsy and machine perfusion. *Am J Transplant.* 2008;8:783–792. doi:10.1111/j.1600-6143.2008.02157.x
6. Port FK, Bragg-Gresham JL, Metzger RA, et al. Donor characteristics associated with reduced graft survival: an approach to expanding the pool of kidney donors. *Transplantation.* 2002;74:1281–1286. doi:10.1097/00007890-200211150-00014
7. Dare AJ, Pettigrew GJ, Saeb-Parsy K. Preoperative assessment of the deceased-donor kidney: from macroscopic appearance to molecular biomarkers. *Transplantation.* 2014;97:797–807. doi:10.1097/01.TP.0000441361.34103.53
8. Vajdová K, Graf R, Clavien P-A. ATP-supplies in the cold-preserved liver: a long-neglected factor of organ viability. *Hepatology.* 2002;36:1543–1552. doi:10.1053/jhep.2002.37189
9. Bruinsma BG, Sridharan GV, Weeder PD, et al. Metabolic profiling during ex vivo machine perfusion of the human liver. *Sci Rep.* 2016;6:22415. doi:10.1038/srep22415
10. Miyagi S, Iwane T, Akamatsu Y, et al. The significance of preserving the energy status and microcirculation in liver grafts from non-heart-beating donor. *Cell Transplant.* 2008;17:173–178. doi:10.3727/000000008783906874
11. Tennankore KK, Kim SJ, Alwayn IP, et al. Prolonged warm ischemia time is associated with graft failure and mortality after kidney transplantation. *Kidney Int.* 2016;89:648–658. doi:10.1016/j.kint.2015.09.002
12. Chouchani ET, Pell VR, James AM, et al. A unifying mechanism for mitochondrial superoxide production during ischemia-reperfusion injury. *Cell Metab.* 2016;23:254–263. doi:10.1016/j.cmet.2015.12.009
13. van Golen RF, van Gulik TM, Heger M. Mechanistic overview of reactive species-induced degradation of the endothelial glycocalyx during hepatic ischemia/reperfusion injury. *Free Radic Biol Med.* 2012;52:1382–1402. doi:10.1016/j.freeradbiomed.2012.01.013
14. Nohl H, Koltover V, Stolze K. Ischemia/reperfusion impairs mitochondrial energy conservation and triggers O<sub>2</sub>– release as a byproduct of respiration. *Free Radic Res Commun.* 1993;18:127–137. doi:10.3109/10715769309147486
15. Lanir A, Jenkins RL, Caldwell C, et al. Hepatic transplantation survival: correlation with adenine nucleotide level in donor liver. *Hepatology.* 1988;8:471–475. doi:10.1002/hep.1840080306
16. Kamiike W, Burdelski M, Steinhoff G, et al. Adenine nucleotide metabolism and its relation to organ viability in human liver transplantation. *Transplantation.* 1988;45:138–143. doi:10.1097/00007890-198801000-00030
17. Grenier N, Pedersen M, Hauger O. Contrast agents for functional and cellular MRI of the kidney. *Eur J Radiol.* 2006;60:341–352. doi:10.1016/j.ejrad.2006.06.024
18. Rusinek H, Kaur M, Lee VS. Renal magnetic resonance imaging. *Curr Opin Nephrol Hypertens.* 2004;13:667–673. doi:10.1097/00041552-200411000-00014
19. Laissy JP, Faraggi M, Lebtahi R, et al. Functional evaluation of normal and ischemic kidney by means of gadolinium-DOTA enhanced TurboFLASH MR imaging: a preliminary comparison with 99Tc-MAG3 dynamic scintigraphy. *Magn Reson Imaging.* 1994;12:413–419. doi:10.1016/0730-725x(94)92534-8
20. Lazeyras F, Buhler L, Vallee J-P, et al. Detection of ATP by “in line” 31P magnetic resonance spectroscopy during oxygenated hypothermic pulsatile perfusion of pigs’ kidneys. *MAGMA.* 2012;25:391–399. doi:10.1007/s10334-012-0319-6
21. Buchs JB, Lazeyras F, Bühler L, et al. The viability of kidneys tested by gadolinium-perfusion MRI during ex vivo perfusion. *Prog Urol.* 2009;19:307–312. doi:10.1016/j.purol.2009.01.004
22. Meier RPH, Piller V, Hagen ME, et al. Intra-abdominal cooling system limits ischemia-reperfusion injury during robot-assisted renal transplantation. *Am J Transplant.* 2018;18:53–62. doi:10.1111/ajt.14399

23. Goujon JM, Hauet T, Menet E, et al. Histological evaluation of proximal tubule cell injury in isolated perfused pig kidneys exposed to cold ischemia. *J Surg Res*. 1999;82:228–233. doi:10.1006/jsre.1998.5526
24. Longchamp A, Meier RPH, Colucci N, et al. Impact of an intra-abdominal cooling device during open kidney transplantation in pigs. *Swiss Med Wkly*. 2019;149:w20143. doi:10.4414/sm.w.2019.20143
25. Moers C, Smits JM, Maathuis MH, et al. Machine perfusion or cold storage in deceased-donor kidney transplantation. *N Engl J Med*. 2009;360:7–19.
26. Kathis JM, Echeverri J, Chun YM, et al. Continuous normothermic ex vivo kidney perfusion improves graft function in donation after circulatory death pig kidney transplantation. *Transplantation*. 2017;101:754–763.
27. Kron P, Schlegel A, de Rougemont O, et al. Short, cool, and well oxygenated—HOPE for kidney transplantation in a rodent model. *Ann Surg*. 2016;264:815–822.
28. Venema LH, Brat A, Nijkamp DM, et al. Factors that complicated the implementation of a program of donation after unexpected circulatory death of lungs and kidneys. lessons learned from a regional trial in the Netherlands. *Transplantation*. 2019;103:e256–e262.
29. Berendsen TA, Izamis ML, Xu H, et al. Hepatocyte viability and adenosine triphosphate content decrease linearly over time during conventional cold storage of rat liver grafts. *Transplant Proc*. 2011;43:1484–1488.
30. Malek M, Nematbakhsh M. Renal ischemia/reperfusion injury; from pathophysiology to treatment. *J Renal Inj Prev*. 2015;4:20–27.
31. de Rougemont O, Breitenstein S, Leskosek B, et al. One hour hypothermic oxygenated perfusion (HOPE) protects nonviable liver allografts donated after cardiac death. *Ann Surg*. 2009;250:674–683.
32. Longchamp A, Mirabella T, Arduini A, et al. Amino acid restriction triggers angiogenesis via GCN2/ATF4 regulation of VEGF and H2S production. *Cell*. 2018;173:117–129.e14.
33. González FX, Rimola A, Grande L, et al. Predictive factors of early post-operative graft function in human liver transplantation. *Hepatology*. 1994;20:565–573.
34. Hamamoto I, Takaya S, Todo S, et al. Can adenine nucleotides predict primary nonfunction of the human liver homograft? *Transpl Int*. 1994;7:89–95.
35. Suntharalingam C, Sharples L, Dudley C, et al. Time to cardiac death after withdrawal of life-sustaining treatment in potential organ donors. *Am J Transplant*. 2009;9:2157–2165.
36. Vidya Shankar R, Kodibagkar VD. A faster PISTOL for 1 H MR-based quantitative tissue oximetry. *NMR Biomed*. 2019;32:e4076.
37. Graveron-Demilly D. Quantification in magnetic resonance spectroscopy based on semi-parametric approaches. *MAGMA*. 2014;27:113–130.